

Excess carbon dioxide as a tracer for air pollution in the Salt Lake Valley during winter time and slope validation of modeled CO:CO₂ emission signatures

Ryan Bares^{1,2}, John Lin¹, Daniel Mendoza¹, Munkhbayar Baasandorj^{1,3}, Sebastian W. Hoch,¹ Ben Fasoli^{1,2}, Logan Mitchell¹

¹Department Atmospheric Sciences, University of Utah, Salt Lake City, UT, USA

²Utah Atmospheric Trace gas and Air Quality Lab, Salt Lake City, UT, USA

³Utah Division of Air Quality, Salt Lake City, UT, USA

Correspondence to: Ryan Bares (ryan.bares@utah.edu)

Abstract Many metropolitan areas in Intermountain West are located in deep valleys that, during periods of sustained high atmospheric stability in winter, can develop Persistent Cold Air Pool (PCAP) events. During these events concentrations of trace gases and fine particulate matter can reach levels that exceed the National Ambient Air Quality Standards (NAAQS). In an effort to understand the relationships between CO₂ and NAAQS criteria pollutants, the Utah Atmospheric Trace gas and Air Quality lab at the University of Utah (U-ATAQ), in conjunction with the Utah Division of Air Quality, took part in an intensive air quality measurement campaign during the winter of 2015 – 2016. Multiple criteria pollutants were measured in-situ, along with high precision carbon dioxide (CO₂) measurements. This period spanned several PCAP events, during which significantly elevated concentrations of pollutants were observed. The excess urban contributions of CO₂ (CO₂exc) and other species were isolated by calculating background mole fractions using a simple but robust mathematical method. A comparison between our mathematical and a differing method that utilizes a “background” measurement site removed from urban influences revealed a highly similar background CO₂ mole fraction constraint during normal atmospheric conditions, but differing concentrations during Persistent Cold Air Pool (PCAP) events. CO₂exc and excess air quality measurements were paired at two different urban locations within the Salt Lake Valley to demonstrate the utility of CO₂exc as a tracer for criteria pollutants, both in and out of PCAPs, where strong correlations were observed. On-road mobile CO and CO₂ measurements were made throughout the Salt Lake Valley over the duration of the sample period providing insight into spatial differences in CO:CO₂ tracer correlations. Mobile data revealed a wide range of relationships likely driven by the presence of near

field emissions, with higher CO:CO₂ ratios on major freeways and lower ratios in residential areas. Finally, we examined the county wide modeled CO:CO₂ emission signature from the most recent version of Hestia, a high-resolution multi-species emission inventory available for Salt Lake City. We found a near systematic overestimation of CO:CO₂ emissions from Hestia by a factor of 2.8, the majority of which results from Hestia's estimation of night time fluxes.

1. Introduction

The Wasatch Front, as well as many other deep basin valleys in the intermountain west, is impacted by Persistent Cold Air Pool (PCAP) events in the winter time, locally known as inversions (Gillies, 2010; *Gorski et al.*, 2015; *Malek* 2006]. PCAP events are multi day episodes of high atmospheric stability driven by synoptic scale high-pressure ridges, and reduced temperatures and insolation associated with wintertime solar angles and surface albedo [*Lareau et al.*, 2014; *Silcox et al.*, 2012; *Whiteman et al.*, 2014]. This persistent atmospheric stability allows for a temperature inversion to develop, which suppresses vertical mixing and allows pollutants to accumulate [*Whiteman et al.*, 2014]. The relationship between PCAP events and elevated pollutant concentrations is well documented [e.g., *Whiteman et al.*, 2010; *Whiteman et al.*, 2014; *Longa et al.*, 2013; *Malek et al.*, 2006]. During PCAP events concentrations of gaseous precursors and fine particulate matter can reach dangerously high levels, well beyond levels set by the National Ambient Air Quality Standards, significantly increasing exposure to PM for the entire population of the impacted valley.

Exposure to fine particulate matter and other air quality pollutants accounts for 6.5 to 7 million global premature deaths annually [*IEA* 2016; *WHO* 2014]. One in eight premature deaths world-wide is attributed to air pollution, making it the fourth deadliest threat to human health. Air pollution exposure has been linked to cardiovascular diseases [*Brugge et al.*, 2007] including stroke and heart disease, respiratory illness like infections [*Kelly and Fussell*, 2011], chronic obstructive pulmonary disease [*Andersen et al.*, 2011] and asthma [*Guarnieri and Balmes*, 2014], as well as childhood development impairments [*Heinrich*, 2007]. The majority of exposure to outdoor air pollution comes from the incomplete combustion of fuels used for energy production. This is particularly

true in urban areas that concentrate people and energy usage, resulting in hot spots of air pollution exposure.

The International Energy Agency calls for the implementation of “A Clean Air Scenario” which is a tailored alternative to current air pollution strategies [2016]. They outline a three part program of setting ambitious long-term air quality goals, implementing clean air policies for energy production sectors, and air quality monitoring, enforcement and evaluation of these policies in order to reduce fatalities and illness associated with air quality pollution.

Despite the scale of air quality impacts and the new called attention to mitigation and monitoring programs, air pollution measurements are generally limited. For instance, the Salt Lake Valley, which has an area of approximately 1,300 km² and a population of 1.03 million residents in 2010, has only one federally regulated NAAQS measurement site that recorded all of the required criteria pollutants (PM_{2.5}, PM₁₀, CO, O₃, SO₂, NO_x, Pb). Thus the exposure rate for the entire population is represented by a single location that does not properly represent the larger geographic extent of the residents. Highly spatially resolved criteria pollutant data are rare, due to the fact that air quality measurements are difficult to make at a high level of precision and accuracy, requiring expensive equipment and highly trained technicians to maintain said equipment.

Carbon dioxide (CO₂) is a long-lived, chemically stable byproduct of fossil fuel combustion co-emitted with various other criteria pollutants including, but not limited to: carbon monoxide (CO), nitrogen oxide (NO), nitrogen dioxide (NO₂), and particulate matter (PM) [Kolb *et al.*, 2004; Watson *et al.*, 1990; Wallington *et al.*, 2008]. Like NAAQS gases, measuring CO₂ to a high degree of accuracy and precision requires a high degree of expensive equipment as well as attention and knowledge. However, CO₂'s primary role in anthropogenic climate forcing has resulted in relatively long-lived and spatially diverse measurement networks. There has been growing interest to measure CO₂ in urban areas [McKain *et al.*, 2012; Mitchell *et al.*, n.d.; Pataki, 2006] due to their significant contributions to global CO₂ emissions. If the relationships between current urban CO₂ trace gas measurements and air pollutants can be well understood, the existing networks of instrumentation can be leveraged as a tool for studying and monitoring air pollution exposure.

One such network is the Utah Urban Carbon Dioxide Network (UUCON), maintained by the Utah Atmospheric Trace Gas and Air Quality lab (U-ATAQ) at the University of Utah. UUCON has six measurement sites distributed throughout the Salt Lake Valley and several additional sites in surrounding valleys, with measurement locations in an array of land uses types [Mitchell *et al.*, n.d. (B)]. Additionally, UUCON measurements began as far back as 2001, offering one of the longest continuous urban CO₂ records available [Mitchell *et al.*, n.d.(A&B)], which provides an unprecedented opportunity to explore CO₂ and air quality relationships. Details regarding sites, measurement methods and historic data can be found in Mitchell *et al.*, [n.d. (B)] and Bares *et al.*, in preparation.

With the population of the Salt Lake Valley expected to double from 2.9 million to 5.4 million residents by 2050 [Harbeke, *et al.*, 2015], accurately predicting the spatial distribution and emission signatures of the associated population growth will be vital in understanding future air pollution exposure rates. Bottom-up emission inventories, which are estimates of the total emissions of greenhouse gases or pollutants for a specific time period and geographic region based on energy consumption, utility and infrastructure data [Gurney *et al.*, 2009; United States Environmental Protection Agency, 2013], will play an important role in predicting the patterns and signatures of future emissions. In order to estimate concentrations and associated exposures, emissions must be transported using a dispersion model [Kuik *et al.*, 2016]. However, emission inventories can serve as a base estimate for predictive mathematical models, the ratios of which can be compared to observed ratios of species.

In this study we looked at the modeled fluxes of CO and CO₂ from Hestia. Hestia is a model with building level spatial resolution capable of estimating fossil fuel emissions based on individual fuel sector (residential, commercial, industrial, on-road) based on available emission inventories [Gurney *et al.*, 2012; Patarasuk *et al.*, 2016]. The current version of Hestia we use for this study has several enhancements including improved building activity and emissions profiles and the addition of three criteria air pollutants: carbon monoxide (CO), nitrogen oxides (NO_x), and fine particulate matter (PM_{2.5}) [Mendoza *et al.*, n.d.]. The ratio of CO₂ emitted with each additional pollutant is unique to individual emission sources [refs], and thus emission signatures vary greatly.

While CO₂ estimates from emission inventories are generally well constrained, with uncertainty ranging from 3% to 40% depending on spatial scale and assimilation methods [Boden *et al.*, 2009; Gurney *et al.*, 2009; Peylin *et al.*, 2009], the unique emission signatures from each source can lead to very high uncertainty when estimating other trace gasses and pollutants. For example, Turnbull *et al.* [2011] compared the ratio of measured fossil fuel-derived CO₂ and other co-measured trace gasses (CO) against available emission inventories and found differences ranging from 200 – 500%.

By understanding the relationships between CO₂ and co-emitted pollutants we can leverage existing CO₂ monitoring infrastructure to expand our spatial and temporal understanding of pollutants. Additionally, we can use the observed relationships, or emission signatures, to compare, validate, and improve existing emission inventories.

The key questions addressed in this study are as follows:

- 1) Is the presence of CO₂exc a good proxy for the presence of NAAQS criteria pollutants CO, NO_x and PM_{2.5}?
- 2) Are the relationships between CO₂exc and criteria pollutants different during PCAP conditions?
- 3) Are the relations between CO₂exc and criteria pollutants consistent across spatial gradients?
- 4) Are the county wide CO:CO₂ emissions predicted by Hestia comparable to those observed? If not what are the likely sources contributing to the error?

2. Methods

2.1 Site Location and Measurement Methods

2.1.1 The Utah Atmospheric Trace gas & Air Quality lab (U-ATAQ) on the University of Utah campus

The U-ATAQ lab is located on the top floor of the eight-story William Browning Building (WBB) on the University of Utah campus, which is situated on the northeastern bench of the Salt Lake Valley, ~150 meters above the valley floor (Figure 1). The inlets for all of the instrumentation in the lab are located on the roof of WBB at 33 meters above ground level. The height of the building, combined with its location above the

valley floor, makes it ideal for measuring atmospheric conditions and tracer concentrations that are more representative of the entire Salt Lake Valley.

The U-ATAQ lab at WBB served as the locus for a larger study aimed at understanding the complex chemistry and atmospheric conditions that lead to the secondary production of particulate matter in the Salt Lake Valley during winter time PCAP events [Baasandorj *et al.*, n.d.]. Measurements began in December of 2015 and ran continuously through the end of February of 2016. Observed species included Carbon Dioxide (CO₂), Carbon Monoxide, (CO), Methane (CH₄), Ozone (O₃), Nitrogen Oxide (NO), Nitrogen Dioxide (NO₂), Nitrogen Trioxide (NO₃), Dinitrogen pentoxide (N₂O₅) Particulate Matter (PM_{2.5}), particle size distributions, particulate chemical analysis, d¹³C and d¹⁸O of CO₂, as well as Meteorological measurements were provided by MesoWest (mesowest.utah.edu) [Horel *et al.*, 2002]. Details regarding each of these analyses can be found in Baasandorj *et al.*, in preparation, Kelly and Martin, in preparation. In this study we choose to limit our analysis to CO₂ and NAAQS criteria pollutants: CO, NO_x, and PM_{2.5}. Other species and measurements will be addressed in *Bassandorj et al.* [in preparation] and *Kelly & Martin* [in preparation].

CO₂ measurements were performed using a Los Gatos Research Off-Axis ICOS (Model 907-0011, Los Gatos Research Inc, San Jose, Ca). Calibration gases were introduced to the analyzer every two hours using three whole-air, high-pressure cylinders with known CO₂ concentrations (tertiary to World Meteorological Organization CO₂ mole fraction scale primaries). Concentrations of standards span the expected range of atmospheric concentrations. Measurements were recorded at 10-sec frequency. Details regarding the calibration materials and post processing of the data can be found in *Bares et al.*, [in preparation].

CO was measured using a Teledyne Advanced Pollution Instrumentation (API) gas filter correlation CO analyzer (Model 300 E, Teledyne API, San Diego, Ca). NO and NO₂ was measured using an API NO_x analyzer (Model T200U). PM_{2.5} mass was measured using an 8500 filter dynamics measurement system (FDMS) – TEOM 1400ab ambient particulate monitor. Details regarding the calibration and data structure of these measurements can be found in *Bassandorj et al.*, [in preparation].

2.1.2 Hawthorne and Sugarhouse

The Utah Department of Environmental Quality maintains the only fully equipped US Environmental Protection Agency (EPA) certified air quality monitoring station in the Salt Lake Valley located at Hawthorne Elementary School (HAW). All EPA regulated criteria pollutants are measured on site in accordance with their specified techniques and calibration protocol, including: CO, NO_x, PM_{2.5}, and O₃. The site is located in a predominantly residential neighborhood, but in close proximity to a busy on-road emission source.

The Sugarhouse (SUG) UUCON CO₂ site is located in the same residential neighborhood as HAW, only 1.3 km to the north east and with a minimal difference in elevation (~20 m). The close proximity to one-another, the similar land use surrounding the sites and the use of hourly averaged data results in strikingly similar measurement profiles between the two locations with diurnal patterns, timing of individual events, and the range of concentrations appearing to be in unison (Figure 3). This data will be referred to as HAW for the remainder of this paper.

Criteria pollutants measured at HAW with the exception of CO were paired with the CO₂ measurements from SUG. During the study period the CO analyzer at HAW experienced numerous problems, including large data gaps during the most intense PCAP event. We chose to exclude CO since the measurements were deemed unreliable, and the lack of data during PCAP events could unintentionally bias results.

2.2 Background and Excess Calculations

All data were averaged from its native frequency into hourly averages. To isolate the urban emissions from the background concentrations, a 24-hour running average was calculated around each hourly data point. The lowest first percentile was calculated for each 24-hour window. This lowest first percentile was chosen to represent the background level for each species, and was subsequently subtracted from the measured mole fraction of each gas to determine the excess concentrations due to urban emissions (Figure 2).

To validate the accuracy of our background estimates, we compared our calculated background constraints against those calculated using methods developed by *Mitchell et al.*, [in preparation (A)], in which CO₂ mole fraction measurements from Hidden Peak (HDP) site were used to represent background constraints. HDP is part of

the Regional Atmospheric Continuous CO₂ Network in the Rocky Mountains (RACCOON) [Stephens et al., 2011] located at 3,351 meters at the top of the Snow Bird ski area. Since this study CO₂ measurements at the site have become the responsibility of U-ATAQ.

Mitchell et al. used CO₂ measurements from HDP that were taken from two inlets and filtered out data that had a difference greater than 0.5 ppm and used observations recorded during the hours of 0000-0500 Local Standard Time (LST) to avoid any potential local fluxes of CO₂. The remaining data was smoothed following the methodology described in *Thoning et al.*, [1989]. This smoothed product was selected as the background constraint.

We found a high degree of agreement between the two methods during times outside of PCAP conditions, but a decoupling of the two methods occurred during PCAP events. Since HDP is removed from the urban component, when PCAP conditions set in and the residence time of emissions increases, urban background significantly rise above that measured at HDP.

Additionally, HDP is limited to measurements of CO₂, and thus can not provide background constraints for the additional criteria pollutants measured in this study. The decoupling between the two sites and the lack of multiple measured species suggests that our calculations are a good way of estimating background conditions in the absence of more intensive methods like those outlined in [Turnbull et al., 2014], which requires timely and expensive collections of flasks for ¹⁴C analysis and can also be species limited.

2.3 Valley Heat Deficit

The Valley Heat Deficit (VHD) is a quantitative, thermodynamic measure of atmospheric stability [Whiteman et al., 2014]. VHD is the amount of heat needed to warm an atmospheric column to a specified height (h) with a 1-m² base to the potential temperature of h, bringing the underlying atmosphere to dry adiabatic lapse rate. Measurements are made using twice a day radinsonde launches at the Salt Lake International Airport (KSLC). Using this method, Whiteman et al. [2014] discovered a threshold of 4 MJ m⁻² (h=2200 meters a.g.l.) heat deficit at which PM_{2.5} concentrations

begin to rise steadily. The relationship between a VHD greater than 4 MJ m^{-2} thus serves as an excellent quantitative indicator of PCAP events.

Since VHD is only measured twice a day from the radiosondes (00 and 12 UTC), values between the launches were linearly interpolated to maintain the hourly data frequency of the trace gas and air pollutant data during PCAP events. Periods when VHD exceeded 4 MJ m^{-2} were isolated from the larger study period and were used to compare observed relationships in and out of PCAP conditions.

2.4 Linear Regressions

To look at relationships between CO_2 and criteria pollutants at individual sites and for inter-site comparison, linear regression analysis was conducted on all species at both locations. Slope of each relationship provides a metric for comparison between locations. All linear regressions were performed using linear model II major axis (MA) regression, which reduces variance in both the X and Y axis, as described by *Legendre & Legendre* [1998] and *Sokal & Rohlf* [1995].

2.5 Mobile sampling

Through the duration of the sample period mobile measurements were performed across the Salt Lake Valley using U-ATAQ's mobile laboratory. Mobile laboratory measurements include CO_2 , CO, CH_4 , O_3 , and NO_x , meteorological measurements, GPS coordinates, as well as ambient air flask collections for laboratory analysis. Details regarding the design of the vehicle can be found in *Bush et al.*, [2012].

For this campaign, CO_2 measurements were made using an LGR UP-GGA, the same model as used for WBB CO_2 measurements. A calibration gas was introduced to the analyzer at the start and end of each transect to account for instrument drift during the drive. CO measurements were conducted using a Picarro G1302 (PICARRO Inc., Santa Clara, CA, USA). The ring-down time on the Picarro during this campaign was substantially degraded, resulting in decreased sample frequency, precision and accuracy. However, the general trends can still lend insight into differences in emission signatures by spatial region when the number of observations (N) per zone is large enough for signal to overcome noise.

A total of 23 independent transects were driven over 11 different days, with the aim of capturing spatial gradients of trace gasses and near surface pseudo-vertical profiles

both in and out of PCAP events (Figure 6). Seven distinct spatial zones of interest were isolated using a complex polygon clip of the underlying trace gas data. These zones include: Interstate 15 ("I15", $N = 19,884$), Interstate 80 ("I80", $N = 2,673$), Interstate 215 ("I215", $N = 10,408$), a residential zone with a large elevational gradient in the Cottonwood Heights neighborhood ("Cottonwood", $N = 7,534$), a historic residential area near the Salt Lake City downtown known as The Avenues ("Aves", $N = 7,589$), and a sparsely developed residential zone with a very large elevational gradient known as the Point of the Mountain ("POM", $N = 17,296$). Linear regression analysis as described in section 2.4 was carried out on each spatial zone to identify an approximate CO:CO₂ emission signature.

2.6 Hestia

The Hestia emissions product for Salt Lake City [Patarasuk *et al.*, 2016] accounts for direct on-site CO₂ emissions from all anthropogenic sectors including on-road, residential, commercial, industrial point, electricity generation, mobile off-road, and commercial point. County emission totals are spatially disaggregated using local data from the department of transportation and federal highway administration, parcel data from the tax assessor data, and population growth and construction activity data. Each sector's emissions were computed independently using temporal traffic profiles and building activity data, and aggregated to produce a total hourly emissions flux for CO₂ and CO. The updated version of the emissions product has three important modifications from the original Hestia. The first modification includes a more realistic heating, ventilation, and air conditioning activity profile for buildings which reflect accepted temperature setpoints during occupied and unoccupied time periods [Mendoza *et al.*, n.d.]. The second modification, also affecting building emissions, is that year-specific meteorology is used to drive the hourly energy consumption patterns as opposed to long-term averaged data used in previous studies [Mendoza *et al.*, n.d.]. The third modification is the inclusion of criteria pollutants, carbon monoxide (CO), nitrogen oxides (NO_x), and fine particulate matter (PM_{2.5}) [Mendoza *et al.*, n.d.].

To examine the temporal structure of CO:CO₂ relationship estimated by Hestia, values were binned hourly then linear regression analysis as outlined in section 2.4 was performed on each bin, resulting in hourly slopes of predicted emission signatures. These

slopes are plotted as a time series, resulting in a diel plot of Hestia predicted CO:CO₂ emissions (Figure 7).

3 Results

3.1 CO₂ as a proxy for Air pollutants

3.1.1 U-ATAQ at William Browning Building

Strong relationships were observed between CO₂exc and all other measured co-emitted pollutants at WBB, both in and out of PCAP events (Table 1, Figure 4). COexc:CO₂exc linear regression revealed a high degree of correlations, with an r² of 0.74 during the entire study period and a slightly lower r² of 0.66 during PCAP events (Figure 4, Table 1). Additionally, the slope of the relationship was near consistent in and out of PCAP conditions, with a slope of 7.40 [ppb/ppm] for the entire sample period and 7.64 during PCAP events. The consistent slope of observed COexc:CO₂exc during significantly different meteorological conditions shouldn't be surprising given the relative stability of both gases.

An even stronger correlation was observed between NOxexc and CO₂exc. With an r² of 0.84 and 0.76 and a slope of 0.88 and 0.90 out and in PCAP conditions respectively (Figure 4, Table 1). The difference in the slopes between PCAP events and the full sample period are likely attributed to the higher degree of reactivity of NOx compared to CO₂, with NOx being on the order of 43,000 times more reactive than CO₂. During PCAP events, the increased residence time of NOx allows for a greater amount of secondary reactions to occur, so the observed concentrations will differ.

The observed relationship between CO₂ and PM_{2.5} is somewhat more complex than the two other discussed co-emitted gaseous pollutants. Particulate matter in urban environments is often the result of secondary reactions of gas phase pollutants suspended in the atmosphere. Thus the relationship between PM and a stable tracer like CO₂ is not necessarily derived from co-emission, but rather from longer-term trends like stable meteorological conditions that allow for the accumulation of pollutants. For instance, multiple studies have identified ammonium nitrate (NH₄NO₃) as a common or dominant component of PM_{2.5} during PCAP events in Northern Utah [Malek *et al.*, 2006, Silva *et al.*, 2007]. Ammonium nitrate is the byproduct of the acid reaction of gas phase nitric

acid (HNO_3), which is formed from NO_2 reacting with O_3 or an OH radical, and gas phase ammonia (NH_3). Thus a series of reactions of emitted gas phase pollutants results in the presence of PM, and not just the direct emission of the particle. Since the concentration of PM during PCAP events is largely impacted by secondary reactions and not just point source emissions, PM concentrations are more homogenous across spatial gradients.

Thus the correlation coefficient (r^2) of $\text{PM}_{2.5\text{exc}}:\text{CO}_{2\text{exc}}$ is exceptionally low when compared to the other species, at 0.17 for the entire sample period.. However during PCAP events, the persistently favorable conditions for secondary cause the relationship to diminish (r^2 0.20), as PM is produced in the atmosphere while CO_2 emissions still only occur as a primary emission (Figure 4).

Since the residence time of pollutants and the secondary production of PM play an important role in the relationship of $\text{PM}_{2.5}$ to CO_2 , when the background level of the pollutants is not removed, thus the total mole fraction (CO_2) and mass concentration ($\text{PM}_{2.5}$) are compared, correlation coefficient is substantially improved to 0.55 for the entire sample period since the background concentrations track well. Thus a potentially useful metric is comparing backgrounds. This relationship results in an r^2 coefficient of 0.87.

3.1.2 Hawthorne

For all gaseous species, the maximum concentrations measured throughout the study and during individual PCAP events were higher at HAW than at WBB. The concentrations of $\text{PM}_{2.5}$ have strikingly similar concentrations throughout the study period suggesting local emissions play less of a role than in the gaseous emissions. Interestingly, the background concentrations in all measured species at both WBB and HAW are highly similar regardless of PCAP strength.

$\text{NO}_{\text{exc}}:\text{CO}_{2\text{exc}}$ relationships reveals a r^2 of 0.50 and 0.49 with a slope of 0.64 and 0.59 out and in PCAP conditions respectively (Figure 5, Table 1). When compared to WBB, the slope and correlation coefficients are very similar for the full sample period; however during PCAP conditions the relationships are slightly different with the slope decreasing at HAW and increasing at WBB during PCAPs.

PM_{2.5}exc:CO₂exc relationships also show a decrease in the measured slope during PCAP events, going from 0.05 during the full sample period down to -0.001 (Figure 5, Table 1). The correlation coefficients are significant lower at HAW with statistically insignificant r² values of .07 and .00 in and out of PCAP events respectively. The substantially weaker correlation seen at HAW than at WBB is likely a result of pairing of data from two different locations. As outlined above, PM is often the result of complex secondary reactions occurring at a larger regional scale. Thus tracer measurements located away from the PM measurements are less likely to be similar than those of gaseous species. Like WBB, the strongest relationship observed between PM_{2.5} and CO₂ is in the background signal (Table 1).

3.2 Mobile Analysis

Slopes of CO:CO₂ collected during mobile on-road sampling identified a clear distinction between highway (I15, I215 and I80) and non-highway (Cottonwood, POM, Aves, Foothill) emission signatures (Figure 6). The average slope of highway spatial zones is 30 while the non-highway average is 21.1. The nature of on-road mobile measurements results in sampling close proximity emission sources, meaning the emission signatures are in part representative of the efficiency of the vehicles near the mobile lab as it travels down a road. When vehicles maintain highway speeds they consume significantly more fuel than while idling at minimum conditions, increasing the relationship between CO and CO₂. Additionally, since the mobile lab is moving while sampling is possible that the air mass being sampled could be a localized plume of higher gaseous concentrations associated with emissions in front of the vehicle.

3.3 Hestia CO:CO₂

By comparing the slopes of the measured (WBB) COexc:CO₂exc to the modeled (Hestia) CO:CO₂ fluxes we can see how well Hestia is doing at estimating the emission signatures in the Salt Lake Valley. Hestia produced a slope of 21.79 for the entire sample period (Figure 7) while the measured slope was 7.4. This indicates that Hestia is over estimating CO emissions by a factor of 2.82. The temporal distribution of CO:CO₂ slopes indicate that the majority of this overestimation occurs while estimating nocturnal emissions (Figure 7). This nocturnal overestimation is likely a result of wood burning for home heating. Since Hestia only accounts for fossil fuel burning when estimating CO₂ it

would fail to incorporate wood burning while the emission inventory derived CO product would. Further work is needed to validate this hypothesis.

4 Conclusions

Excess carbon dioxide appears to be a good indicator of co-emitted primary criteria pollutants. CO_2^{exc} shows strong and consistent relationships across multiple locations with other emitted trace gasses (CO and NO_x). The lack of reliable CO data from HAW during this study is unfortunate, but given the strength of the observed $\text{CO}_2^{\text{exc}}:\text{NO}_x^{\text{exc}}$ and the similarity to that observed at WBB, it is not unreasonable to expect a similarly strong result.

As seen at WBB, CO_2 mole fraction does a reasonable job at indicating the presence of $\text{PM}_{2.5}$. However this relationship breaks down as PCAP conditions facilitate secondary atmospheric reactions that result in the formation of PM. Additionally, concentrations of gaseous species appear to be more influenced by local emissions while PM is more spatially homogenous. This is evident by the higher concentrations in gaseous species measured at HAW than at WBB, while the PM measurements are highly similar. This can also account for CO_2^{exc} failure to capture a similar $\text{PM}_{2.5}$ relationship in the HAW data set since the CO_2 measurements are not co-located.

The choice of background constraint is highly important when making these kinds of comparisons. Our mathematical constraint shows strength in several ways. It found a high degree of agreement with background measurement sites when similar atmospheric conditions persist. It is able to account for the decoupling of backgrounds when PCAP events drive elevated backgrounds in urban settings. It is applicable to multiple species and different data frequencies. And finally, it does not require additional expensive and time intensive measurements.

While the absolute values of the CO measurements from the mobile van used in this analysis are not highly reliable, the number of observations per spatial zone allows us to compare relative relationships. Our mobile measurements indicate large differences in the emission signatures of freeway and non-freeway areas, with freeway zones consistently producing slopes 50% higher than non-freeway zones.

When compared to our in-situ measurements we find that Hestia is currently overestimating the emission of CO to CO₂ by a factor of close to 3. As demonstrated in figure 7, this appears to be largely driven by overestimations of CO:CO₂ fluxes during night time, indicating that Hestia's failure to account for wood burning by the home heating sector may be a significantly contribution to the error.

While excess carbon dioxide does a good job at indicating the presence of gaseous pollutants, and in some cases fine particulate matter, these relationships will be spatially dependent as a result of significant variations in emission sources within an urban domain. In order to best leverage existing trace gas infrastructure more work is needed to understand and quantify these relationships at each measurement location. Mobile data and high resolution emission inventories like Hestia can help inform these relationships, but both of these products have certain uncertainties that limit their effectiveness. Thus, high quality, co-located measurements, both in and out of PCAP conditions, would be best to capture these relationships and begin to utilize the long term and spatially diverse CO₂ infrastructure that currently exists along the Wasatch Front.

References Cited

- Andersen, Z. J., Hvidberg, M., Jensen, S. S., Ketzel, M., Loft, S., Sørensen, M., ... Raaschou-Nielsen, O. (2011). Chronic obstructive pulmonary disease and long-term exposure to traffic-related air pollution: A cohort study. *American Journal of Respiratory and Critical Care Medicine*, 183(4), 455–461.
- Baasandorj et al., (n.d.)
- Bares, R.B., Fasoli, N., Lin., L.C., Bowling, D., Ehleringer, J.R., Catharine, D., Eng, B., Garcia, M. (n.d.). University of Utah's improvements to the Utah urban carbon dioxide network: Instrumentation, sample design and stability.
- Brugge, D., Durant, J. L., & Rioux, C. (2007). Near-highway pollutants in motor vehicle exhaust: A review of epidemiologic evidence of cardiac and pulmonary health risks. *Environmental Health*, 6(1), 1–12. <http://doi.org/10.1186/1476-069X-6-23>
- Boden, T. A., Marland, G., and Andres, R. J.: Global, regional and national fossil-fuel CO₂ emissions, Carbon Dioxide Information Analysis Center, Oak Ridge National Laboratory, US Department of Energy, Oak Ridge, Tenn., USA, 2009
- Brugge, D., Durant, J. L., & Rioux, C. (2007). Near-highway pollutants in motor vehicle exhaust: A review of epidemiologic evidence of cardiac and pulmonary health risks. *Environmental Health*, 6(1), 1–12. <http://doi.org/10.1186/1476-069X-6-23>
- Bush, S.E., Hopkins, F.M., Randerson, T.J., Ehleringer, J. R. (2012). Design and application of a mobile ground-based observatory for continuous measurements of atmospheric trace gas and criteria pollutant species S. *Atmospheric Measurement Techniques*, 28, 63–86. <http://doi.org/10.1016/j.cognition.2008.05.007>
- Gillies, R. R., Wang, S.-Y., & Booth, M. R. (2010). Atmospheric Scale Interaction on Wintertime Intermountain West Low-Level Inversions. *Weather and Forecasting*, 25(4), 1196–1210. <http://doi.org/10.1175/2010WAF2222380.1>
- Gorski, G., Strong, C., Good, S. P., Bares, R., Ehleringer, J. R., & Bowen, G. J. (2015). Vapor hydrogen and oxygen isotopes reflect water of combustion in the urban atmosphere. *Proceedings of the*

- National Academy of Sciences of the United States of America*, 112(11).
<http://doi.org/10.1073/pnas.1424728112>
- Guarnieri, M., & Balmes, J. R. (2014). Outdoor air pollution and asthma. *The Lancet*, 383(9928), 1581–1592. [http://doi.org/10.1016/S0140-6736\(14\)60617-6](http://doi.org/10.1016/S0140-6736(14)60617-6)
- Gurney, K. R., Mendoza, D. L., Zhou, Y., Fischer, M. L., Miller, C. C., Geethakumar, S., and de la Rue du Can, S.: High resolution fossil fuel combustion CO₂ emission fluxes for the United States, *Environ. Sci. Technol.*, 43, 5535–5541, doi:10.1021/es900806c, 2009.
- Gurney, K. R., Zhou, Y., Mendoza, D., Chandrasekaran, V., Geethakumar, S., Razlivanov, I., ... Godbole, a. (2011). Vulcan and Hestia: High resolution quantification of fossil fuel CO₂ emissions. *MODSIM 2011 - 19th International Congress on Modelling and Simulation - Sustaining Our Future: Understanding and Living with Uncertainty*, (December), 1781–1787.
- Harbecke, D. T., Garbett, B., Chairman, V., Matsumori, D., Kroes, S. J. H., & City, S. L. (2014). A Snapshot of 2050, (720).
- Heinrich, J., & Slama, R. (2007). Fine particles, a major threat to children. *International Journal of Hygiene and Environmental Health*, 210(5), 617–622. <http://doi.org/10.1016/j.ijheh.2007.07.012>
- Horel, J., M. Splitt, L. Dunn, J. Pechmann, B. White, C. Ciliberti, S. Lazarus, J. Slemmer, D. Zaff, and J. Burks (2002), Mesowest: cooperative mesonets in the western United States, *Bull. Am. Meteorol. Soc.*, 83, 211–225.
- International Energy Agency. (2016). Energy and Air Pollution. *World Energy Outlook - Special Report*, 266. <http://doi.org/10.1021/ac00256a010>
- Kelly, F. J., & Fussell, J. C. (2011). Air pollution and airway disease. *Clinical and Experimental Allergy*, 41(8), 1059–1071. <http://doi.org/10.1111/j.1365-2222.2011.03776.x>
- Kelly, K., Martin, R. (n.d)
- Kolb, C. E., S. C. Herndon, J. B. McManus, J. H. Shorter, M. S. Zahniser, D. D. Nelson, J. T. Jayne, M. R. Canagaratna, and D. R. Worsnop (2004), Mobile Laboratory with Rapid Response Instruments for Real-Time Measurements of Urban and Regional Trace Gas and Particulate Distributions and Emission Source Characteristics, *Environ. Sci. Technol.*, 38, 5694–5703.
- Lareau, N. P., Crosman, E., Whiteman, C. D., Horel, J. D., Hoch, S. W., Brown, W. O. J., & Horst, T. W. (2013). The persistent cold-air pool study. *Bulletin of the American Meteorological Society*, 94(1), 51–63. <http://doi.org/10.1175/BAMS-D-11-00255.1>
- Legendre, P., & GALLAGHER, E. I. Legendre. 1998. Numerical ecology. *Second English Edition. Elsevier, New York.*
- Longa, R. W., Eatough, N.L., Mangelson, N.F., Thompson, W., Fiet, K., Smith, S., Smith, R., Eatough, D.J., Pope, C.A., Wilson, W.E., 2003. The measurement of PM_{2.5}, including semi-volatile components, in the EMPACT program: results from the Salt Lake City Study. *Atmos. Env.* 37 (31), 4407e4417.
- Malek, E., Davis, T., Martin, R. S., & Silva, P. J. (2006). Meteorological and environmental aspects of one of the worst national air pollution episodes (January, 2004) in Logan, Cache Valley, Utah, USA. *Atmospheric Research*, 79(2), 108–122. <http://doi.org/10.1016/j.atmosres.2005.05.003>
- McKain, K., S. C. Wofsy, T. Nehrkorn, J. Eluszkiewicz, and J. Ehleringer (2012), Assessment of ground-based atmospheric observations for verification of greenhouse gas emissions from an urban region, *Proc. Natl. Acad. Sci.*, 109(22), 8423–8428.
- Mitchell, L. E. et al. A (n.d.), Long-term urban carbon dioxide observations reveal spatial and temporal dynamics related to urban form and growth, *Proc. Natl. Acad. Sci.*
- Mitchell, L.E., et al. B (n.d.), The Salt Lake City, USA Urban Carbon Dioxide Monitoring Network
- Pataki, D. (2006), Urban ecosystems and the North American Carbon Cycle, *Glob. Chang. Biol.*, 12, 2092–2101.
- Peylin, P., Houweling, S., Krol, M. C., Karstens, U., Rødenbeck, C., Geels, C., Vermeulen, A., Badawy, B., Aulagnier, C., Pregger, T., Delage, F., Pieterse, G., Ciais, P., and Heimann, M.: Importance of fossil fuel emission uncertainties over Europe for CO₂ modeling: model intercomparison, *Atmos. Chem. Phys. Discuss.*, 9, 7457–7503, doi:10.5194/acpd-9-7457-2009, 2009.
- Silcox, G. D., Kelly, K. E., Crosman, E. T., Whiteman, C. D., & Allen, B. L. (2012). Wintertime PM_{2.5} concentrations during persistent, multi-day cold-air pools in a mountain valley. *Atmospheric Environment*, 46, 17–24. <http://doi.org/10.1016/j.atmosenv.2011.10.041>

- Silva, P. J., Vawdrey, E. L., Corbett, M., & Erupe, M. (2007). Fine particle concentrations and composition during wintertime inversions in Logan, Utah, USA. *Atmospheric Environment*, *41*(26), 5410–5422. <http://doi.org/10.1016/j.atmosenv.2007.02.016>
- Sokal, R. R., & Rohlf, F. J. (1995). Assumptions of analysis of variance. *Biometry: The principles and practice of statistics in biological research*, 392–450.
- Stephens, B. B., Miles, N. L., Richardson, S. J., Watt, A. S., & Davis, K. J. (2011). Atmospheric CO₂ monitoring with single-cell NDIR-based analyzers. *Atmospheric Measurement Techniques*, *4*(12), 2737–2748. <http://doi.org/10.5194/amt-4-2737-2011>
- Turnbull, J. C., Karion, A., Fischer, M. L., Faloona, I., Guilderson, T., Lehman, S. J., ... Tans, P. P. (2011). Assessment of fossil fuel carbon dioxide and other anthropogenic trace gas emissions from airborne measurements over Sacramento, California in spring 2009. *Atmospheric Chemistry and Physics*, *11*(2), 705–721. <http://doi.org/10.5194/acp-11-705-2011>
- Thoning, K. W., P. P. Tans, and W. D. Komhyr (1989), Atmospheric carbon dioxide at Mauna Loa Observatory: 2. Analysis of the NOAA GMCC data, 1974–1985, *J. Geophys. Res. Atmospheres*, *94*(D6), 8549–8565, doi:10.1029/JD094iD06p08549.
- United States Environmental Protection Agency (2013). ANNEX 2 Methodology and Data for Estimating CO₂ Emissions from Fossil Fuel Combustion, 29–125.
- Wallington, T. J., Sullivan, J. L., & Hurley, M. D. (2008). Emissions of CO₂, CO, NO_x, HC, PM, HFC-134a, N₂O and CH₄ from the global light duty vehicle fleet. *Meteorologische Zeitschrift*, *17*(2), 109–116. <http://doi.org/10.1127/0941-2948/2008/0275>
- Watson, R. T., Rodhe, H., Oeschger, H., & Siegenthaler, U. (1990). Greenhouse gases and aerosols. *Climate Change: The IPCC Scientific Assessment*, 1–40. Retrieved from <http://www.scopus.com/inward/record.url?eid=2-s2.0-0025587274&partnerID=40&md5=5d3e969d5d655f48f55e679627df52ab>
- Whiteman, C.D., Hoch, S.W., Lehiner, M. (2010). Nocturnal cold-air intrusions into a closed basin: Observational evidence and conceptual model. *Journal of applied meteorology and climatology*, *49*, 1894–1905.
- Whiteman, C. D., Hoch, S. W., Horel, J. D., & Charland, A. (2014). Relationship between particulate air pollution and meteorological variables in Utah’s Salt Lake Valley. *Atmospheric Environment*, *94*, 742–753. <http://doi.org/10.1016/j.atmosenv.2014.06.012>
- WHO. (2014). WHO ’s Ambient Air Pollution database - Update 2014 Data summary of the AAP database, 2–7. Retrieved from http://www.who.int/phe/health_topics/outdoorair/databases/cities/en/

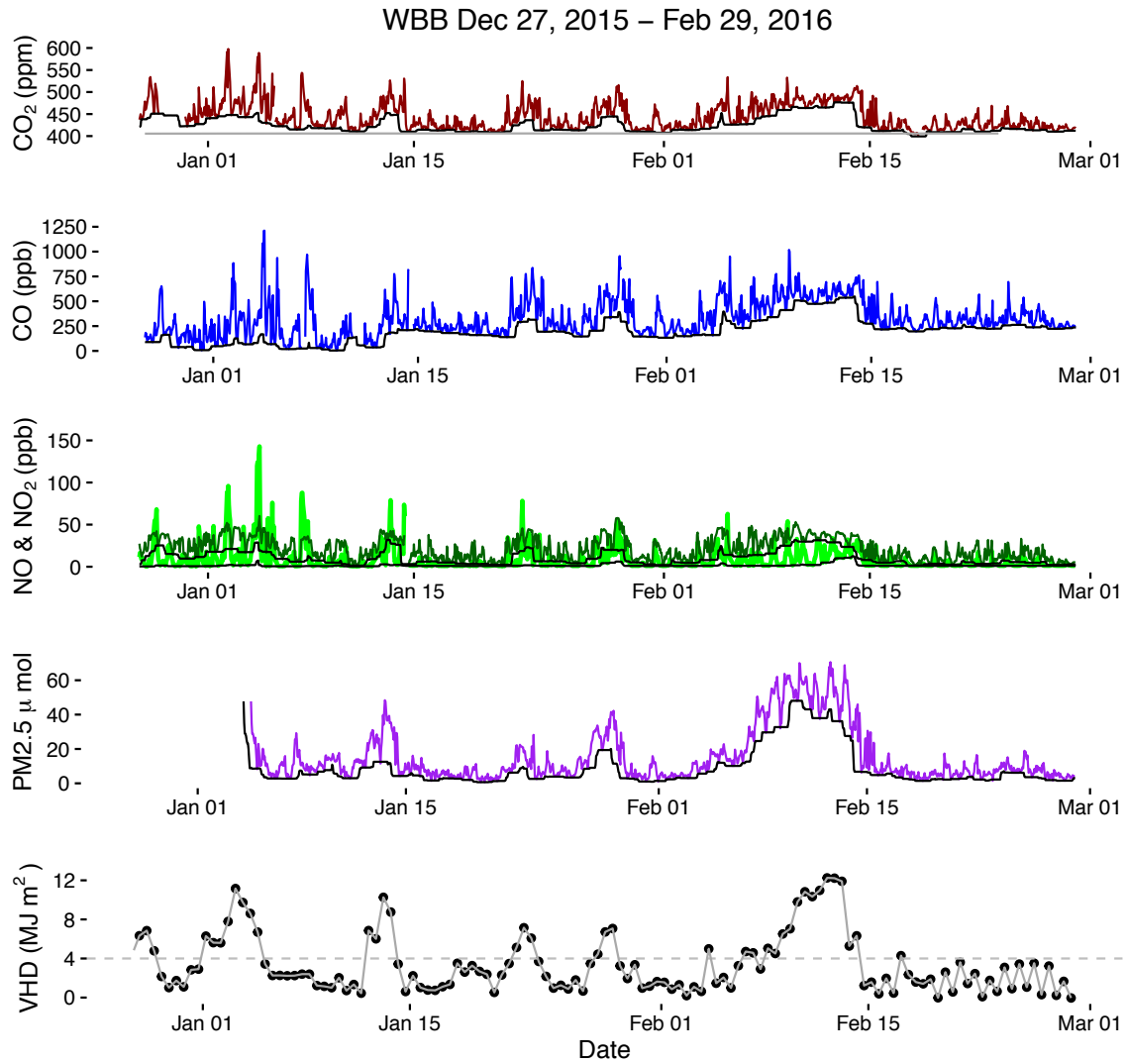


Figure 2 Time series of measurements from WBB with CO₂ in red, CO in blue, NO in light green, NO₂ in dark green in the same field, PM_{2.5} in purple and the VHD in gray with black dots in the bottom field. Black lines are our mathematically derived background constraint. Gray line in the CO₂ field is the Mitchell et al., background product derived from measurements at HDP.

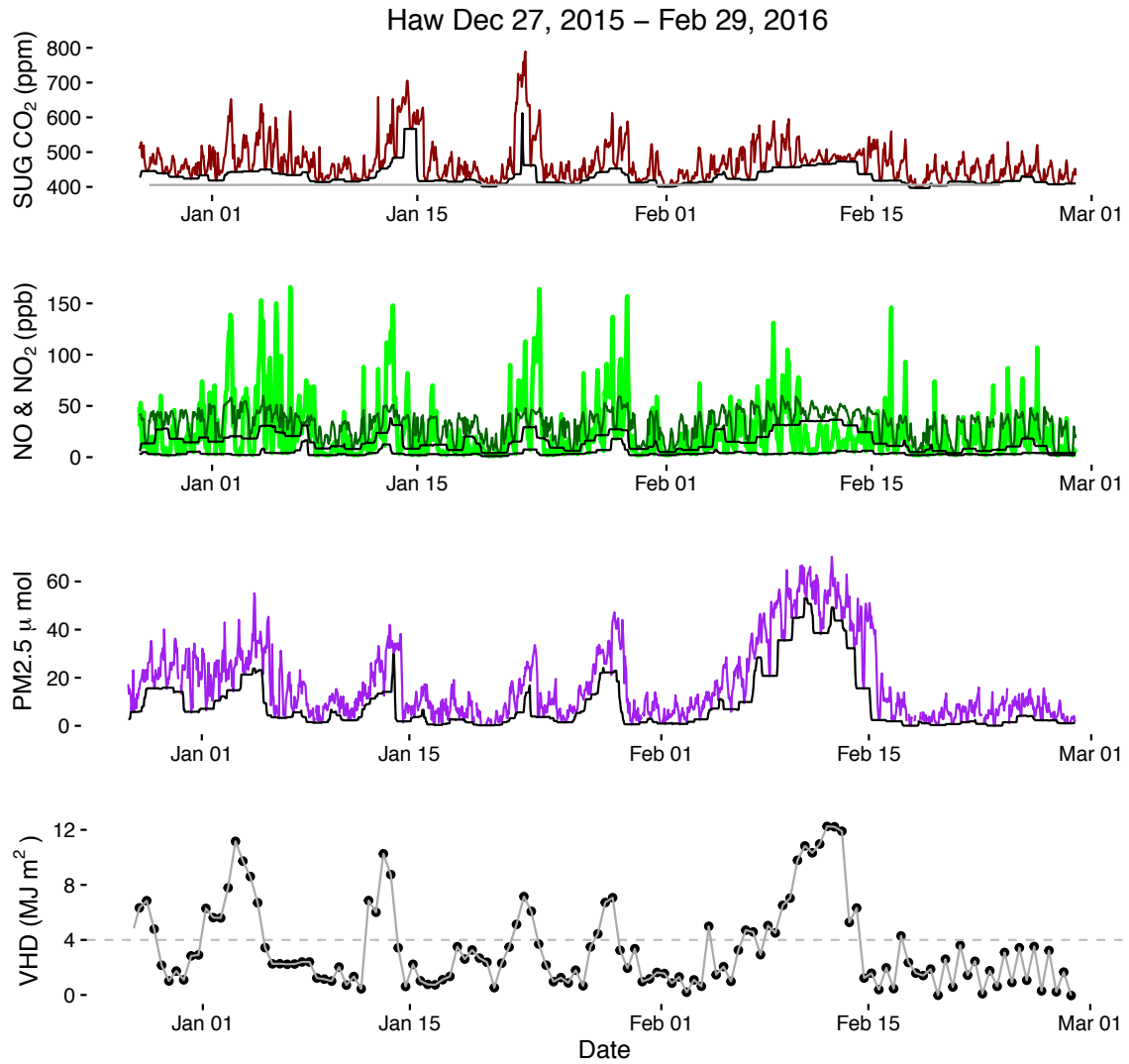


Figure 3 Time series of measurements from HAW with CO₂ in red, CO in blue, NO in light green, NO₂ in dark green in the same field, PM_{2.5} in purple and the VHD in gray with black dots in the bottom field. Black lines are our mathematically derived background constraint.

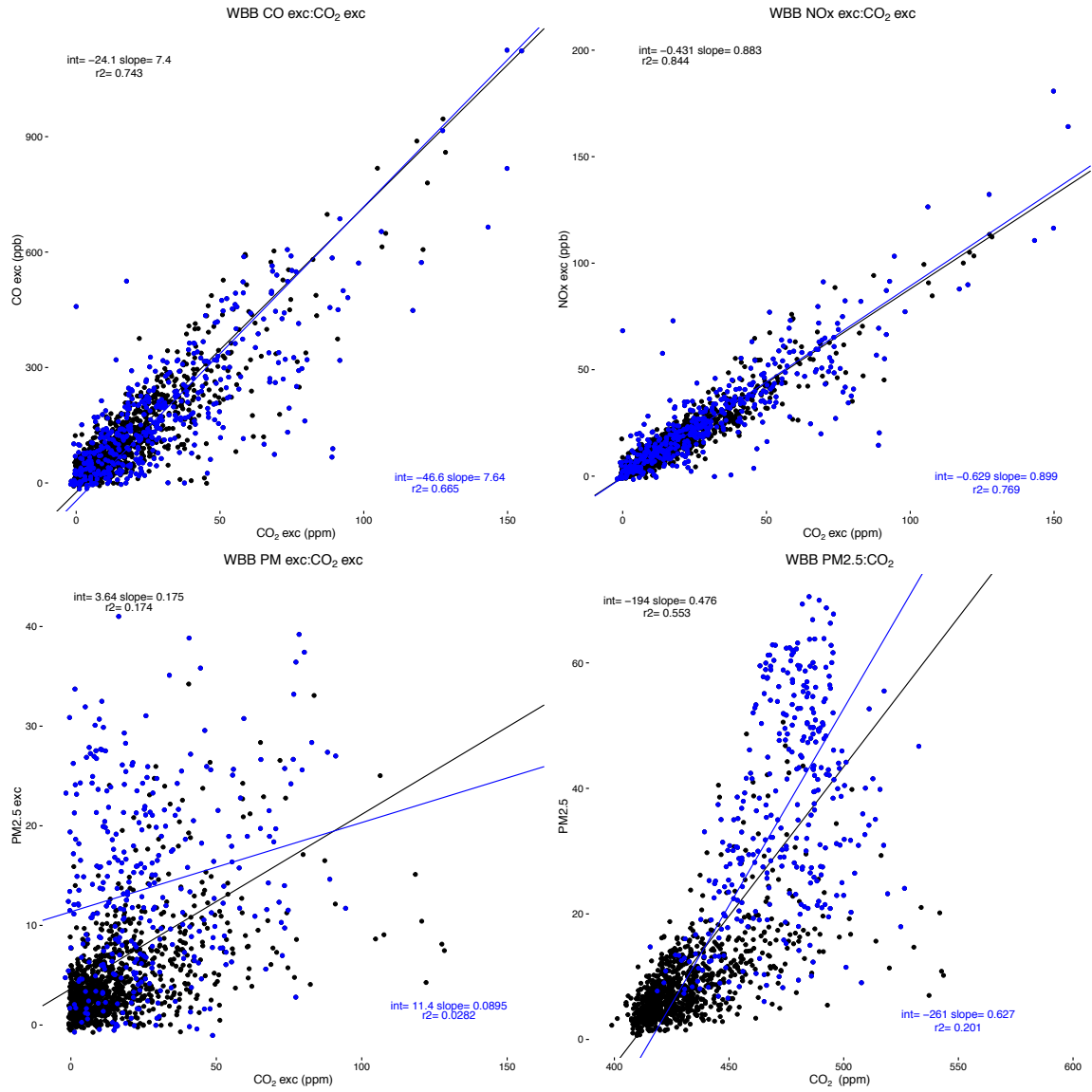


Figure 4 WBB linear relationships. Black dots represent the full sample period where blue are periods during PCAP conditions.

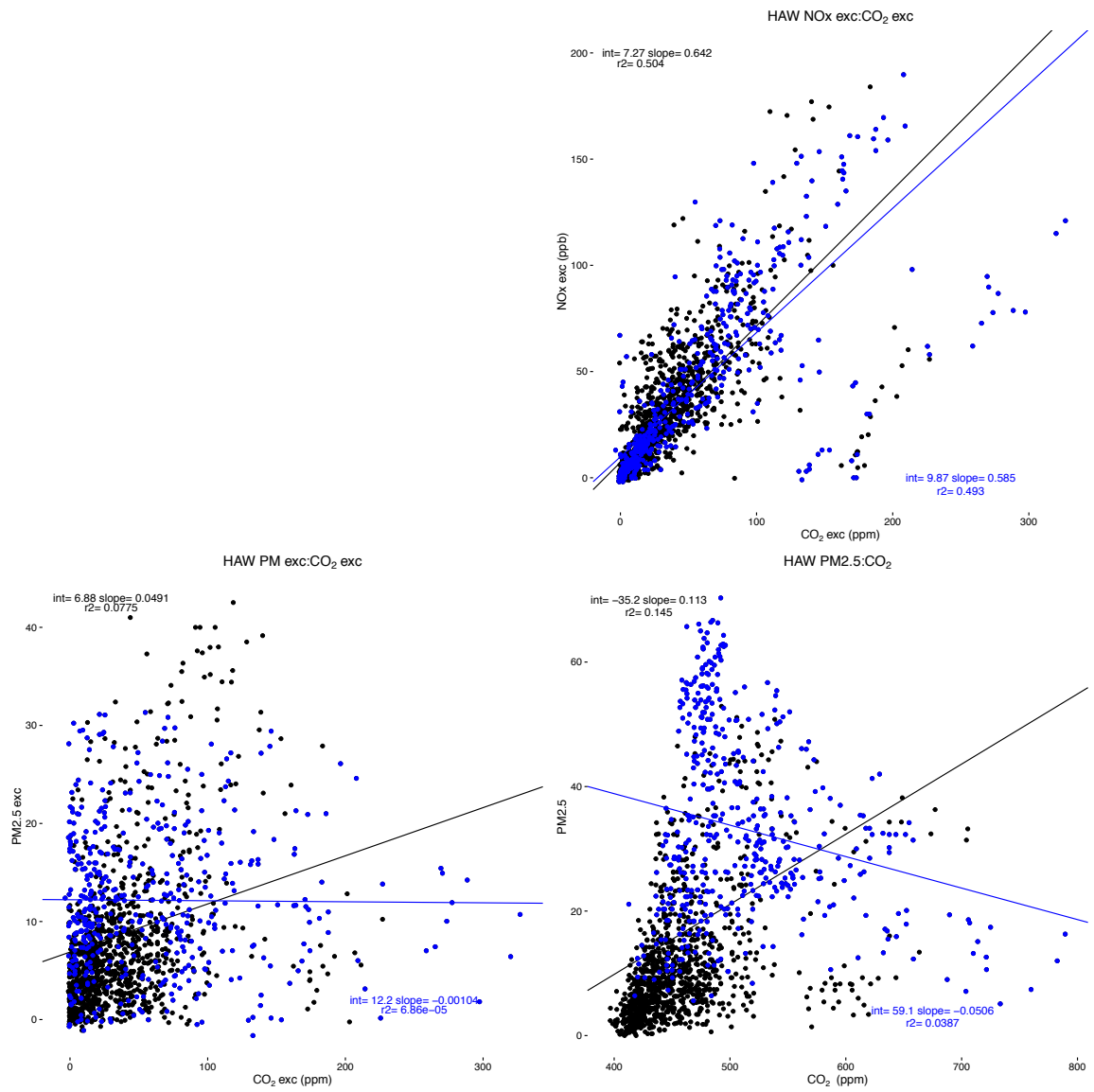


Figure 5 HAW linear relationships. Black dots represent the full sample period where blue are periods during PCAP conditions.

Table1: Slopes and correlation coefficients

	WBB Slope	WBB r ²	HAW Slope	HAW r ²	Hestia Slope	Hestia r ²
CO _{exc} :CO _{2exc}	7.40	0.743			21.79*	0.701
PCAP CO _{exc} :CO _{2exc}	7.64	0.665				
NO _{xexc} :CO _{2exc}	.0.883	0.844	0.642	0.504		
PCAP NO _{xexc} :CO _{2exc}	0.899	0.769	0.585	0.493		
PM _{2.5exc} :CO _{2exc}	0.175	0.174	0.049	0.077		
PCAP PM _{2.5exc} :CO _{2exc}	0.089	0.028	-0.001	0.00		
PM _{2.5} :CO ₂ Mole Fraction	0.476	0.201	0.113	0.145		
PCAP PM _{2.5} :CO ₂ Mole Fraction	0.627	0.201	-0.05	0.038		
PM _{2.5} :CO ₂ Background	0.598	0.868	0.288	0.319		

*** Flux estimate**

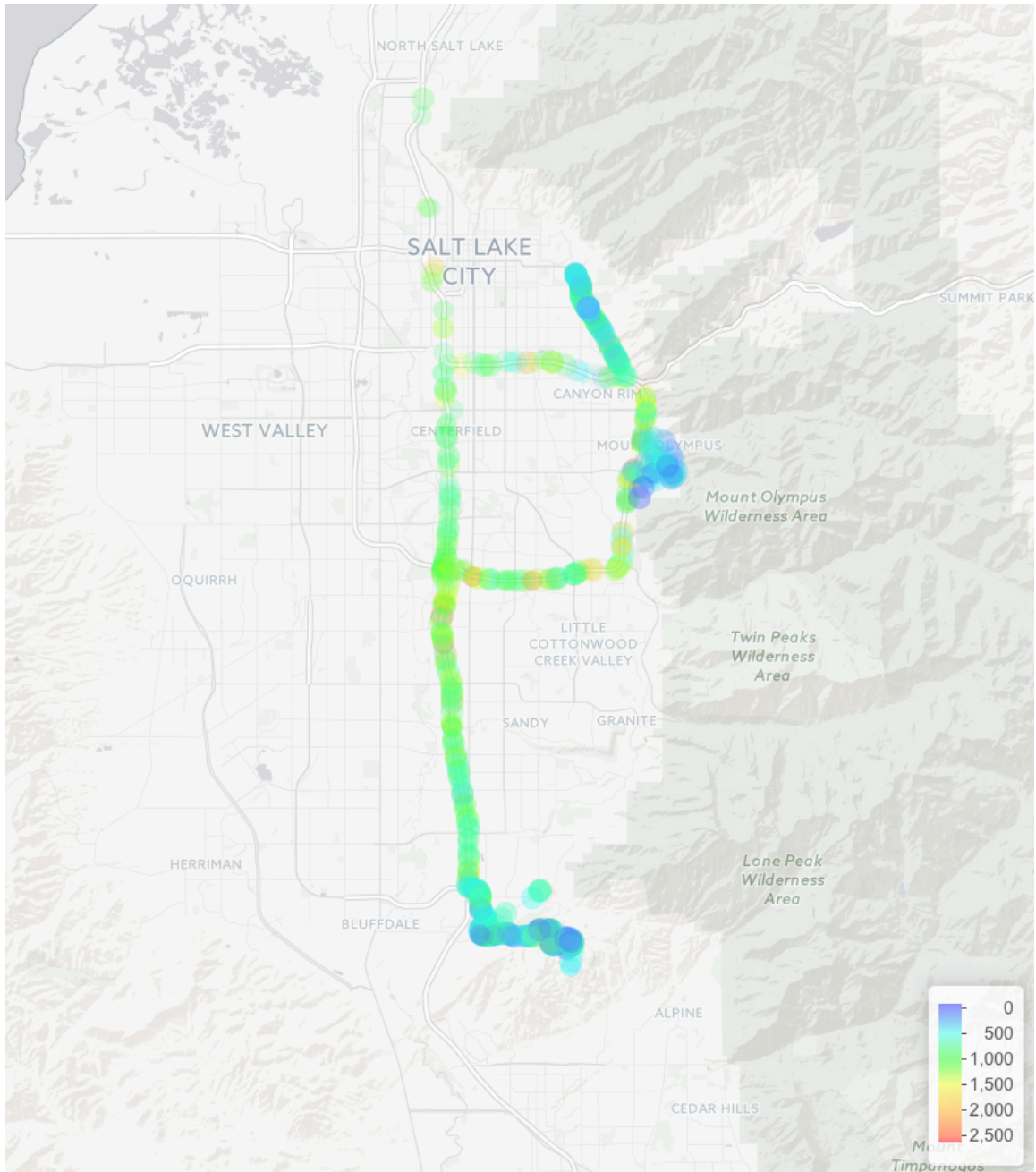


Figure 6 Map of mobile CO ppb measurements throughout campaign after sub-setting for spatial zones of interest. You can see distinctly higher CO ppb on freeways compared to non-freeway areas.

Hestia & WBB Slopes by Hour

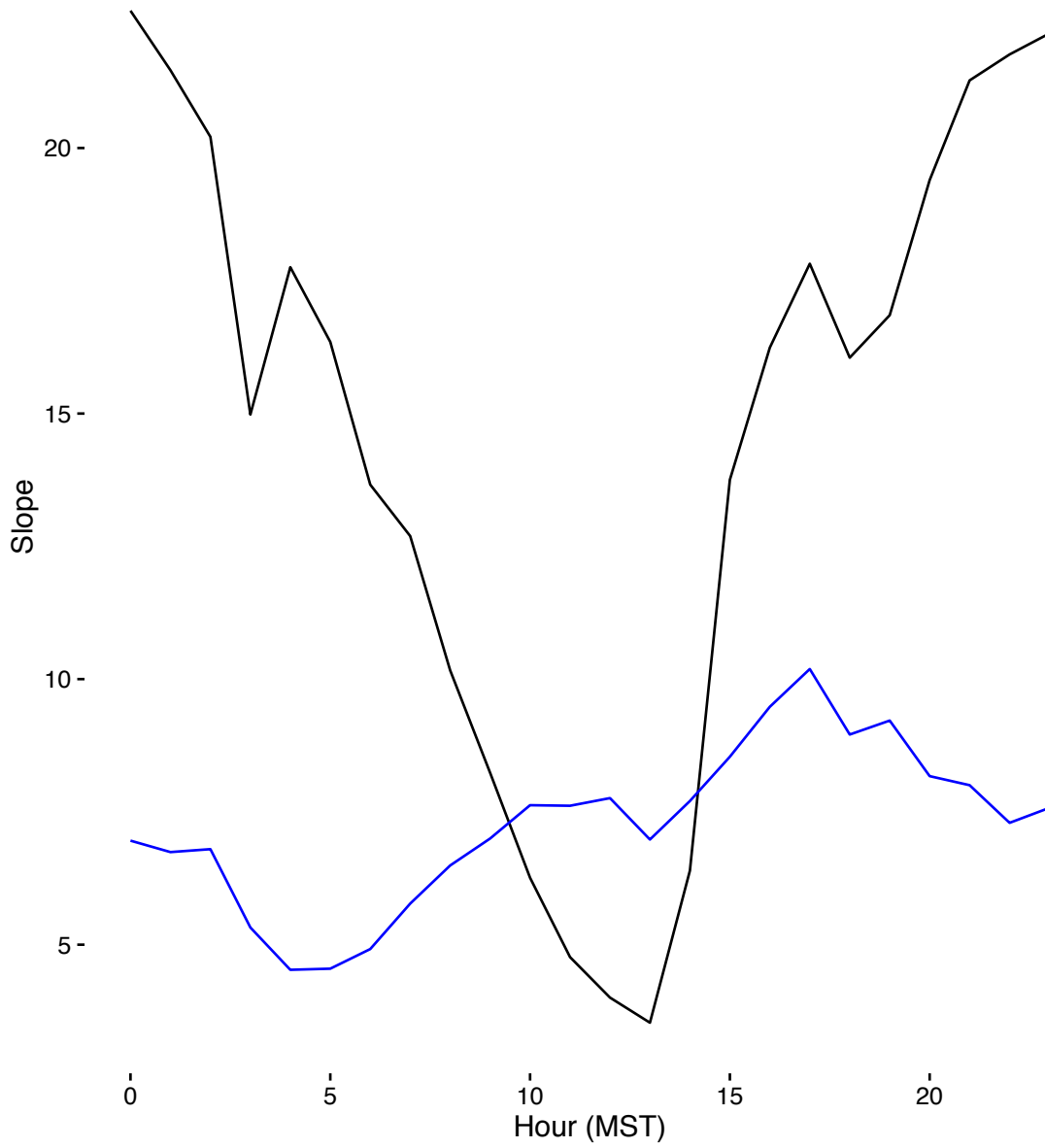


Figure 7 Hestia predicted (black) and WBB observed (blue) CO:CO₂ slopes as binned by hour. The nocturnal overestimation of CO is very apparent.